Clinical and Experimental Obstetrics & Gynecology

Clin. Exp. Obstet. Gynecol. **2025**; 52(9): 42387
https://doi.org/10.31083/CEOG42387

Original Research

Application of Microvascular-Flow Imaging to Characterize Placental Microvascularization in Preeclamptic and Healthy Pregnancies

Jianmei Peng[1], Yangyang Fan[2], Liang Mu[1], Li Liu[1], Meiqing He[1], Yanhua Gao[1], Jing Shang[1], Xixi Zhang[1,*]

[1]Department of Ultrasound, Shaanxi Provincial People's Hospital, 710068 Xi'an, Shaanxi, China
[2]Department of Obstetrics, Shaanxi Provincial People's Hospital, 710068 Xi'an, Shaanxi, China
*Correspondence: xixizhang1989@163.com (Xixi Zhang)

Academic Editor: Paolo Ivo Cavoretto
Submitted: 23 May 2025 Revised: 19 July 2025 Accepted: 23 July 2025 Published: 24 September 2025

Abstract

Background: Preeclampsia (PE) is a common pregnancy complication and involves placental dysfunction and ischemia. Microvascular-Flow (MV-Flow) imaging was utilized to quantitatively assess placental microvascular architecture in PE. MV-Flow was also used to compare the microvascular architecture between PE and normal pregnancies, as well as between early- and late-onset PE cases. **Methods**: The study enrolled 87 consecutive singleton pregnancies that underwent MV-Flow imaging examination between June 2021 and December 2021. Among these, 50 were normotensive pregnancies and 37 were PE pregnancies. The PE group was further stratified into early-onset (<34 weeks gestational age [GA], n = 25) and late-onset (≥34 weeks GA, n = 12) subtypes. Among the 50 normal cases, 38 were <34 weeks, and 12 were ≥34 weeks. MV-Flow technology was used to measure the placental vascular index (VI^{MV}). The VI^{MV}s for the middle and peripheral placental segments were referred to as VI^{MV}-m and VI^{MV}-p, respectively. Placental VI^{MV}s were compared between PE and normotensive pregnancies, as well as between early- and late-onset PE cases. Perinatal outcomes were evaluated in pregnancies complicated by PE. A p-value < 0.05 (two-sided) was considered to be statistically significant. **Results**: No significant difference between the VI^{MV}-p and VI^{MV}-m was observed in either the normotensive or PE group, and neither parameter correlated with GA. Both VI^{MV}-p and VI^{MV}-m were significantly lower in early-onset PE cases compared to normotensive pregnancies <34 weeks GA ($p < 0.001$). Similarly, late-onset PE cases also showed lower VI^{MV}-p and VI^{MV}-m compared to normotensive pregnancies ≥34 weeks GA ($p < 0.001$). No significant differences were observed between early- and late-onset PE cases in either VI^{MV}-p ($p = 0.170$) or VI^{MV}-m ($p = 0.471$). Among PE pregnancies, placental VI^{MV} measurements revealed no significant differences between appropriate-for-GA (AGA) and small-for-GA (SGA) neonates (VI^{MV}-p: 21.40 [17.70–27.30] *vs.* 21.50 ± 2.50, $p = 0.949$; VI^{MV}-m: 21.30 [17.50–27.50] *vs.* 22.80 ± 6.40, $p = 0.881$). **Conclusions**: MV-Flow imaging enables quantitative assessment of microvascular architecture in PE placentas. Both early- and late-onset PE pregnancies showed significantly lower placental VI^{MV} compared to normotensive pregnancies, supporting the clinical utility of MV-Flow for the evaluation of placental perfusion in PE. Furthermore, no significant difference in placental VI^{MV} was observed between early- and late-onset PE, suggesting a similar impairment of placental perfusion in both subtypes.

Keywords: placenta; preeclampsia; pregnancy; ultrasonography

1. Introduction

Preeclampsia (PE) is a common pregnancy complication affecting 3%–8% of pregnancies globally [1,2]. It remains a leading cause of maternal and perinatal morbidity and mortality [1,2]. Worldwide, approximately 10 million women develop PE annually, resulting in an estimated 76,000 maternal deaths and 500,000 neonatal deaths attributable to PE-related hypertensive disorders [1,3]. According to the American College of Obstetricians and Gynecologists, the principal diagnosis of PE is the onset of hypertension after 20 weeks of gestation, accompanied by signs of end-organ damage including proteinuria, thrombocytopenia, renal insufficiency, impaired liver function, pulmonary edema, or new-onset headache/visual symptoms that are unresponsive to medication and unexplained by alternative diagnoses [4]. Clinically, PE is stratified into early-onset (<34 weeks of gestation) and late-onset (≥34 weeks of gestation) subtypes based on the gestational age (GA) at disease onset [5].

Placental perfusion is associated with both maternal blood flow and fetal circulation. Physiologically, trophoblast invasion induces remodeling of maternal uterine spiral arteries, characterized by loss of the vascular muscular layer and subsequent vasodilation. This transformation establishes high-flow uteroplacental circulation through the structural conversion of uterine arteries into low-resistance vessels [1,6,7]. The pathophysiology of early-onset PE stems primarily from defective spiral artery remodeling, leading to impaired uteroplacental perfusion, defective placentation, and subsequent placental hypoxia [8,9]. In contrast, late-onset PE is associated with placental oxidative changes triggered by progressive disparity between maternal perfusion and fetoplacental demands [8,9]. While the pathogenesis and placental pathology of early- and late-

Copyright: © 2025 The Author(s). Published by IMR Press.
This is an open access article under the CC BY 4.0 license.

Publisher's Note: IMR Press stays neutral with regard to jurisdictional claims in published maps and institutional affiliations.

onset PE appear to be different, both forms involve placental dysfunction and ischemia [9,10].

Given the central role of the placenta in PE pathophysiology, it is important to develop non-invasive, clinically practical methods for its *in vivo* functional assessment [11,12]. In terms of conventional ultrasonography, Doppler parameters for the umbilical artery (UA) and uterine artery (UtA) provide overall resistive indices for the upstream arterial vessels of placental vascular beds on the fetal and maternal sides, respectively. However, these metrics only provide an indirect assessment of placental perfusion and cannot directly quantify microvascular density within the placenta [13]. Therefore, more advanced non-invasive imaging modalities capable of direct visualization and quantitative assessment of placental microvascular perfusion characteristics may be required [14].

Previous studies have attempted to assess placental perfusion using three-dimensional (3D) power Doppler ultrasound. However, this approach is limited by factors such as equipment settings, the requirement for experienced operators, and low reproducibility in the second and third trimesters [13,14]. Recently, a new and non-invasive microvascular-flow (MV-Flow) imaging technology (Samsung Medison Co. Ltd, Seoul, Korea) has been used to assess the microvasculature in carotid plaque, hepatic parenchyma, fetal brain, and the placenta in normal, fetal growth restriction, and placenta accreta spectrum disorders [13]. Thanks to key features including high tissue suppression (noise reduction), advanced flash artifact filtering, compound imaging capabilities, and high sensitivity, MV-Flow technology can detect minute vessels with low-velocity blood flow that are not visible with conventional Doppler imaging [15,16]. This innovative technology not only enables visualization of the placental villous shaft, but also quantification of the placental microvascular structure at the level of the villous lobe [17].

The aim of the present study was to evaluate the utility of MV-Flow imaging in characterizing the placental microvascular architecture in PE pregnancies. In addition, considering the distinct pathophysiological pathways between early- and late-onset PE, we compared microvascular differences between PE and normal pregnancies, as well as between early- and late-onset PE cases.

2. Materials and Methods

2.1 Patients

The protocol for this observational study was approved by the institutional review board of the hospital from which cases were recruited. Written informed consent was obtained from all participating subjects.

The study enrolled 87 consecutive pregnant women who underwent ultrasound examination in our department between June 2021 and December 2021. Placental MV-flow imaging was performed on all cases. The following inclusion criteria were applied: singleton pregnancy, healthy pregnant women without any gestation-related disease, pregnant women diagnosed with PE, successful ultrasound examination, an anterior placenta, and GA $>$20 weeks as determined from the last menstrual period and ultrasound measurements. PE was diagnosed according to established criteria of the American College of Obstetricians and Gynecologists [4]. The exclusion criteria were: fetal chromosomal/structural anomalies, placental implantation abnormalities (placenta previa, bilobed placenta, or placenta accreta spectrum disorders), and umbilical cord insertion anomalies (marginal $<$2 cm from edge, or velamentous insertion) [18].

Of the 87 singleton pregnancies that were finally included, 50 were normal cases without PE (normal group) and 37 were PE cases (PE group). The mean maternal age was 29.60 $\pm$ 4.90 years (range, 21–42 years), while the mean GA was 31.40 $\pm$ 4.00 weeks. Within the PE group, cases were stratified by GA at diagnosis into early-onset ($<$34 weeks GA, n = 25) and late-onset ($\geq$34 weeks GA, n = 12) subtypes. Among the 50 normal cases, 38 were $<$34 weeks GA, and 12 were $\geq$34 weeks GA.

2.2 Ultrasound Imaging

Ultrasound examinations were performed using a HERA W10 ultrasound system (Samsung Medison Co., Ltd., Seoul, Korea) equipped with a transabdominal CA1–7 MHz transducer. All scans were conducted by a maternal-fetal medicine-certified sonographer with $>$15 years of specialized obstetric ultrasound experience. The protocol for transabdominal ultrasound examination included: evaluation of fetal biometry; evaluation of fetal anatomy; evaluation of the localization of the placenta; pulsed Doppler studies of the UA, bilateral UtAs and middle cerebral artery (MCA); placental microvascular quantification via MV-Flow imaging technology [18]. Artery waveforms for MCA, UA, and UtAs were obtained by pulsed Doppler imaging. For each artery, the resistive index (RI) and pulsatility index (PI) were measured when three consecutive similar waveforms were present [19].

In this study, when the fetus was not moving, maternal breath-holding was practiced to allow acquisition of an optimal placental gray image, after which the MV-Flow function was activated to obtain a stable MV-Flow image of the placenta. For each case, the MV-Flow examination parameters were set as follows: image quality: normal; sensitivity: 26; tissue suppression: 3; color gain: 50; filter: 3; smooth: 1; LumiFlow: 2; alpha blending: 75%; dynamic range: 20 [13]. Once the MV-Flow function was activated, the placental microvasculature image was shown and an ellipse-shaped region of interest (ROI) was automatically provided. The ROI size was modified to envelope as much of the placental microvasculature as possible. This included placental chorionic vessels only, and excluded vessels located within the uterine muscles or on the surface of the chorionic plate. Subsequently, the vascular index (VI^{MV})

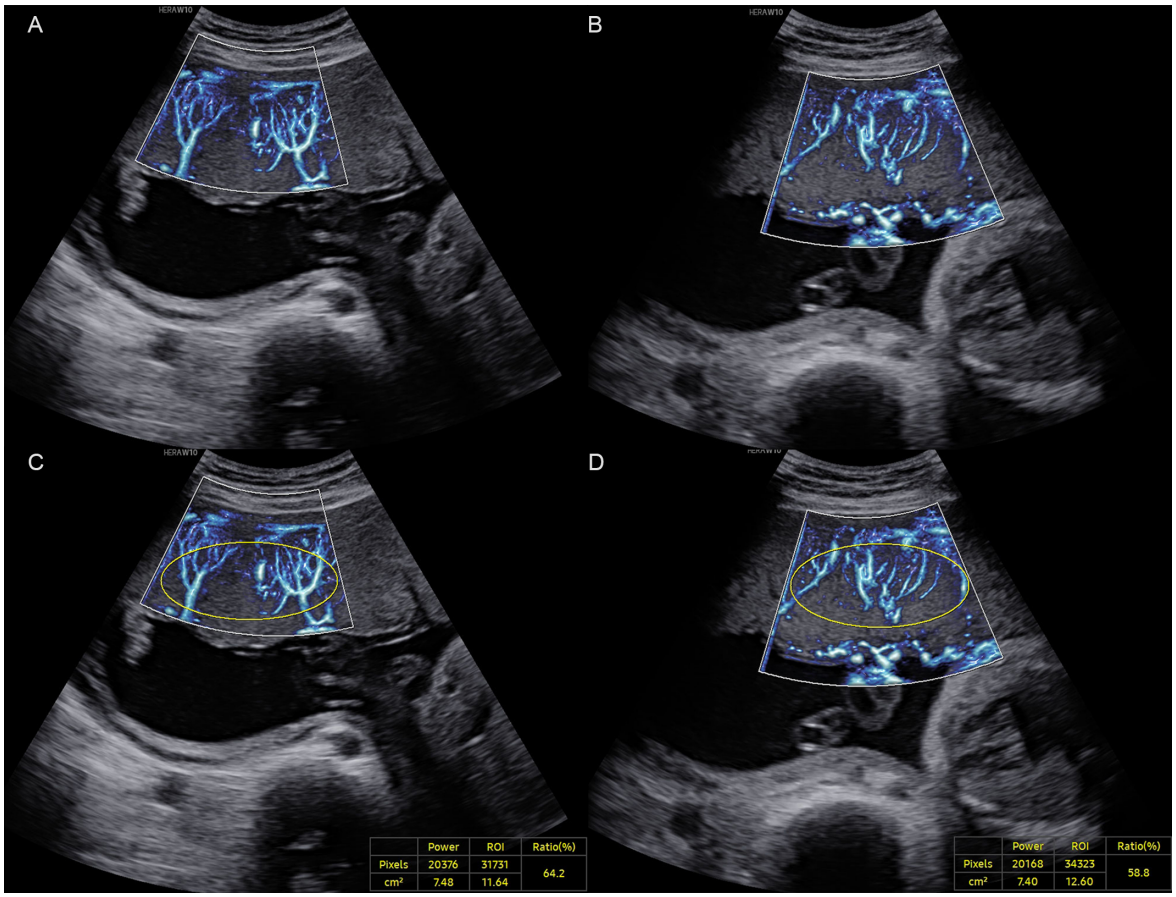

Fig. 1. A normal pregnancy case at 27^{+6} weeks of gestation. (A) MV-Flow imaging of the peripheral segment of the placenta along the longitudinal axis. (B) MV-Flow imaging of the middle segment. (C) Vascular index (VI^{MV}) for the peripheral segment (VI^{MV}-p, 64.2%). (D) VI^{MV} for the middle segment (VI^{MV}-m, 58.8%). ROI, region of interest; MV-Flow, microvascular-flow. The yellow circle shows the ellipse-shaped region of interest for which the VI^{MV} was calculated.

for the ROI was automatically calculated by the software. The VI^{MV}, defined as the ratio of the number of blood-filled pixels to total pixels within the ultrasound image, allowed the microvascularization per region of biological tissue to be quantified. Therefore, placental VI^{MV} represents a quantitative assessment of placental microvascularization.

The placenta was divided into middle and peripheral regions along the longitudinal axis, with the middle segment corresponding to the middle third of the placenta along its axis, and the peripheral segment comprising the remaining portion [20]. MV-Flow imaging was performed three times in both the middle and peripheral placental segments, yielding three separate VI^{MV} measurements per region. The mean of three measurements per region was calculated and recorded as VI^{MV}-middle (VI^{MV}-m) or VI^{MV}-peripheral (VI^{MV}-p) (Fig. 1).

2.3 Follow-up of PE Pregnancies

Pregnancy outcome data were collected for pregnant women diagnosed with PE. The following perinatal outcomes were recorded: GA at delivery, mode of delivery, birthweight and birthweight percentile, and Apgar test score. The 2015 Chinese neonatal birth weight curve for different GA [21] was used to classify newborns according to their birthweight. Those with a birthweight below the 10th percentile were defined as small for gestational age (SGA), while neonates with a birthweight between the 10th and 90th percentile were defined as appropriate for gestational age (AGA) [19].

2.4 Statistical Analyses

The Shapiro-Wilk test was used to assess whether the sample data was normally distributed. Continuous data were presented as the mean $\pm$ standard deviation (SD) if it was normally distributed, and as the median (interquartile range, IQR) if it showed non-normal distribution. Categorical data were presented as percentages and frequencies. Statistical analysis was performed with Fisher exact, Student *t*, Mann-Whitney U, and Kruskal-Wallis tests, as appropriate. A p-value < 0.05 (two-sided) was considered to be statistically significant. Statistical analyses were performed with SPSS Statistics for Windows (version 27.0; SPSS Inc., Chicago, IL, USA).

Table 1. Comparison of placental VI^{MV} between PE and normal pregnancies.

	PE (n = 37)	Normal pregnancy (n = 50)	*p*
Maternal age (years)	31.40 ± 5.50	28.30 ± 3.90	0.005
GA at examination (weeks)	32.20 ± 3.40	30.80 ± 4.30	0.102
VI^{MV}-p (%)	19.90 (18.40–24.70)	42.80 ± 8.50	<0.001
VI^{MV}-m (%)	21.20 (17.30–27.40)	42.40 ± 8.10	<0.001

n represents the sample size. PE, preeclampsia; GA, gestational age.

3. Results

Among the 87 cases included in this study, 50 were normal pregnancies and 37 were diagnosed with PE. Women with PE were significantly older than healthy controls (31.40 ± 5.50 *vs.* 28.30 ± 3.90 years; $p = 0.005$; Table 1). At the time of ultrasound examination, the GA of the normal group (30.80 ± 4.30 weeks) was not significantly different to that of the PE group (32.20 ± 3.40 weeks; $p = 0.102$; Table 1).

The intra-observer correlation coefficients for VI^{MV}-m and VI^{MV}-p were 0.96 (95% confidence interval (CI): 0.94–0.97) and 0.94 (95% CI: 0.92–0.96), respectively, demonstrating the high reliability of measurements.

In normal pregnancies, no significant difference was observed between the VI^{MV}-p and VI^{MV}-m (42.80 ± 8.50 *vs.* 42.40 ± 8.10, $p = 0.556$). Moreover, neither the VI^{MV}-p nor the VI^{MV}-m was correlated with GA ($p = 0.410$ and 0.086, respectively). Similarly, in PE pregnancies, no significant difference was observed between the VI^{MV}-p (19.90 [18.40–24.70]) and VI^{MV}-m (21.20 [17.30–27.40], $p = 0.829$), and neither parameter was correlated with GA ($p = 0.455$ and 0.207, respectively).

VI^{MV} values for the control and PE groups were compared irrespective of the GA. Both the VI^{MV}-p and VI^{MV}-m in the PE group were significantly lower than those in the control group ($p < 0.001$; Table 1).

GA at examination was <34 weeks in 63 cases (38 normal and 25 early-onset PE cases), and ≥34 weeks in 24 cases (12 normal and 12 late-onset PE cases). For cases <34 weeks, no significant difference in GA was observed between the normal and early-onset PE groups ($p = 0.115$; Table 2). However, the early-onset PE group exhibited significantly lower VI^{MV}-p and VI^{MV}-m values compared to normal controls ($p < 0.001$; Table 2). For cases ≥34 weeks, no significant difference in GA was observed between the normal and late-onset PE groups ($p = 0.779$; Table 3). However, the late-onset PE group also showed significantly lower VI^{MV}-p and VI^{MV}-m values compared to the normal group ($p < 0.001$; Table 3; Fig. 2). No significant differences in placental VI^{MV}-p ($p = 0.170$) or VI^{MV}-m ($p = 0.471$) were found between early- and late-onset PE cases.

Hemodynamic parameters for the UA, bilateral UtAs, and MCA were compared between PE cases and GA-matched normal cases. In the early-onset PE group, the RI and PI of the UA and of both UtAs were significantly higher than those of the normal group at <34 weeks GA ($p < 0.05$; Table 2). In contrast, the MCA-RI was significantly lower ($p < 0.05$; Table 2). In the late-onset PE group, UA-RI and UA-PI were elevated compared to normal cases ≥34 GA ($p < 0.05$; Table 3), but no significant differences were observed between the two groups for the UtA or MCA hemodynamic parameters ($p > 0.05$; Table 3). The centiles of UA-PI and UtA-PI according to GA were further evaluated against recently published reference ranges (Tables 2,3) [22,23].

Perinatal outcomes were systematically evaluated in pregnancies complicated by PE. In the 37 PE cases, two early-onset cases were lost to follow-up, while three early-onset cases underwent medically indicated pregnancy termination. All 32 remaining PE cases (20 early-onset and 12 late-onset) underwent cesarean delivery at our institution, allowing comprehensive analysis of perinatal outcomes including GA at delivery, birth weight, and Apgar scores (1-, 5-, and 10-minute) (Table 4). The Apgar scores at 1 and 5 minutes were significantly higher in the late-onset PE group than in the early-onset PE group ($p < 0.001$ and $p = 0.039$, respectively). Based on birth weight and GA at delivery, 24 neonates were classified as AGA and 8 as SGA. No significant differences in placental vascular indices were observed between the AGA and SGA groups: VI^{MV}-p (21.40 [17.70–27.30] *vs.* 21.50 ± 2.50, $p = 0.949$), and VI^{MV}-m (21.30 [17.50–27.50] *vs.* 22.80 ± 6.40, $p = 0.881$).

4. Discussion

This study utilized MV-Flow ultrasound technology to quantify placental microvascularization, expressed as VI^{MV}, in both normal and PE pregnancies. Our findings revealed significantly reduced placental VI^{MV} values in PE pregnancies compared to normal pregnancies. Compared with normal pregnancies of <34 weeks GA, early-onset PE cases exhibited significantly lower placental VI^{MV}, as well as greater hemodynamic resistance in both UtAs and UA. Compared with normal pregnancies of ≥34 weeks GA, late-onset PE cases demonstrated lower VI^{MV} and higher UA resistance; however, no significant difference was observed in the resistance of UtAs between these groups.

We found no difference between the VI^{MV}-p and VI^{MV}-m in either the PE or normal groups, demonstrating that placental VI^{MV} was not related to the measure-

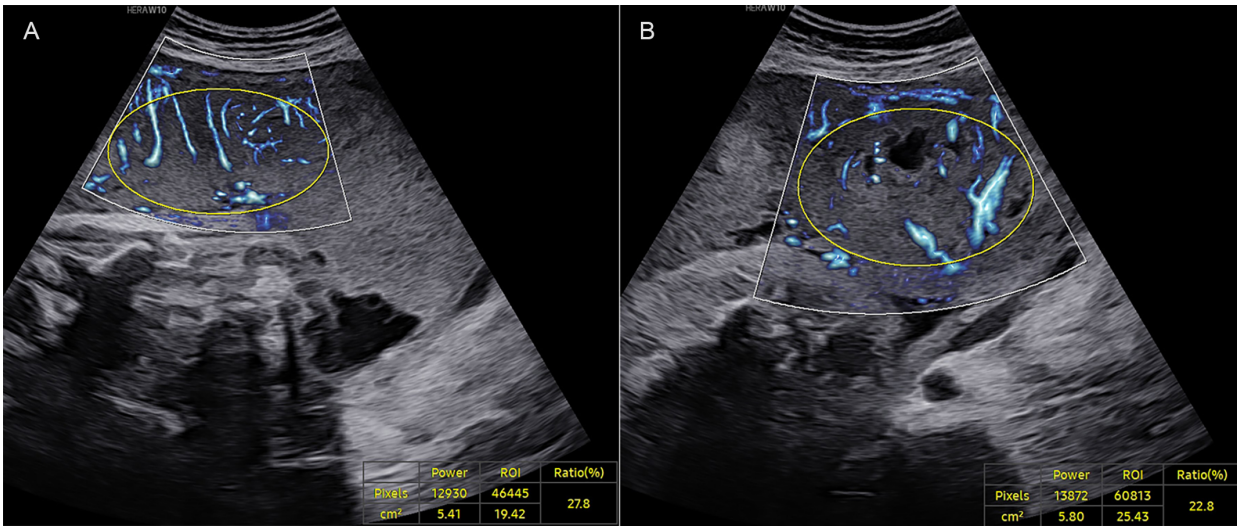

Fig. 2. A late-onset PE case at 37^{+0} weeks of gestation. (A) VI^{MV} for the middle segment (VI^{MV}-m, 27.8%). (B) VI^{MV} for the peripheral segment (VI^{MV}-p, 22.8%). The yellow circle shows the ellipse-shaped region of interest for which the VI^{MV} was calculated.

Table 2. Comparison of placental VI^{MV} and hemodynamic characteristics between early-onset PE and normal pregnancies at <34 weeks of gestation.

	Early-onset PE (n = 25)	Normal pregnancy <34 weeks GA (n = 38)	*p*
GA (weeks)	30.20 ± 2.00	28.60 (27.10–31.30)	0.115
VI^{MV}-p (%)	19.00 (17.30–23.40)	42.10 ± 8.50	<0.001
VI^{MV}-m (%)	19.80 (17.30–25.10)	40.70 (37.00–46.20)	<0.001
Umbilical artery			
RI	0.72 ± 0.16	0.63 ± 0.08	0.013
PI	1.16 (0.86–1.45)	0.96 ± 0.18	0.030
Middle cerebral artery			
RI	0.78 ± 0.09	0.85 ± 0.06	0.002
PI	1.68 (1.24–1.87)	1.88 ± 0.41	0.066
Right uterine artery			
RI	0.76 (0.59–0.84)	0.48 ± 0.09	<0.001
PI	1.84 (1.01–2.25)	0.68 (0.53–0.87)	<0.001
Left uterine artery			
RI	0.68 ± 0.13	0.48 ± 0.08	<0.001
PI	1.26 (0.99–2.16)	0.70 (0.60–0.82)	<0.001
GA-specified centile of UA-PI (n)			0.022
<10th	4/25 (16%)	6/38 (16%)	
10th–90th	11/25 (44%)	30/38 (79%)	
>90th	10/25 (40%)	2/38 (5%)	
GA-specified centile of right UtA-PI (n)			<0.001
<10th	0/25 (0%)	11/38 (29%)	
10th–90th	9/25 (36%)	25/38 (66%)	
>90th	16/25 (64%)	2/38 (5%)	
GA-specified centile of left UtA-PI (n)			<0.001
<10th	0/25 (0%)	7/38 (18%)	
10th–90th	9/25 (36%)	30/38 (79%)	
>90th	16/25 (64%)	1/38 (3%)	

PI, pulsatility index; RI, resistive index; UA-PI, umbilical artery pulsatility index; UtA-PI, uterine artery pulsatility index.

Table 3. Comparison of placental VI^{MV} and hemodynamic characteristics between late-onset PE and normal pregnancies at ≥34 weeks of gestation.

	Late-onset PE (n = 12)	Normal pregnancy ≥34 weeks GA (n = 12)	*p*
GA (weeks)	36.20 ± 1.50	36.50 ± 2.10	0.779
VI^{MV}-p (%)	23.50 ± 5.10	45.00 ± 8.40	<0.001
VI^{MV}-m (%)	22.80 ± 6.70	43.80 ± 8.50	<0.001
Umbilical artery			
RI	0.61 ± 0.08	0.51 ± 0.06	0.004
PI	0.93 ± 0.19	0.71 ± 0.13	0.003
Middle cerebral artery			
RI	0.75 (0.74–0.78)	0.78 ± 0.09	0.416
PI	1.41 (1.31–1.50)	1.64 ± 0.39	0.116
Right uterine artery			
RI	0.48 ± 0.11	0.44 (0.39–0.48)	0.470
PI	0.69 (0.54–0.85)	0.63 (0.54–0.71)	0.419
Left uterine artery			
RI	0.49 ± 0.15	0.51 ± 0.12	0.673
PI	0.63 (0.50–1.04)	0.83 ± 0.31	0.460
GA-specified centile of UA-PI (n)			0.039
<10th	1/12 (8%)	5/12 (42%)	
10th–90th	8/12 (67%)	7/12 (58%)	
>90th	3/12 (25%)	0/12 (0%)	
GA-specified centile of right UtA-PI (n)			0.832
<10th	2/12 (17%)	1/12 (8%)	
10th–90th	9/12 (75%)	10/12 (84%)	
>90th	1/12 (8%)	1/12 (8%)	
GA-specified centile of left UtA-PI (n)			0.746
<10th	3/12 (25%)	1/12 (8%)	
10th–90th	6/12 (50%)	8/12 (67%)	
>90th	3/12 (25%)	3/12 (25%)	

Table 4. Perinatal outcomes in preeclamptic pregnancies.

	Early-onset PE (n = 20)	Late-onset PE (n = 12)
Maternal age (years)	32 ± 5	30 ± 5
GA at examination (weeks)	30.50 ± 1.70	36.20 ± 1.50
Birth age (weeks)	31.30 ± 2.20	36.30 ± 1.50
Birth weight (g)	1429.00 ± 441.00 (960.00–2480.00)	2321.00 ± 468.00 (1410.00–3020.00)
Birth classification (n)		
SGA newborn	3/20 (15%)	5/12 (42%)
AGA newborn	17/20 (85%)	7/12 (58%)
Sex (n)		
Female	8/20 (40%)	8/12 (67%)
Male	12/20 (60%)	4/12 (33%)
Apgar score at 1 min	6.70 ± 2.50 (range, 1–10)	9 for 7 cases, 10 for 5 cases
Apgar score at 5 min	2 for one case, 9 for 5 cases, 10 for 14 cases	10 for all cases
Apgar score at 10 min	2 for one case, 9 for 3 cases, 10 for 16 cases	10 for all cases

SGA, small for gestational age; AGA, appropriate for gestational age.

ment site. Both VI^{MV}-m and VI^{MV}-p showed high intra-observer agreement, with correlation coefficients of 0.96 and 0.94, respectively. These results indicate that placental VI^{MV} could be a highly reproducible metric, regardless of the sampling location. Chen *et al.* [13] also previously evaluated the placental microvascular architecture in nor-

mal and fetal growth-restricted pregnancy with MV-Flow imaging. In agreement with the present study, these workers found no significant variation in VI^{MV} among different placental regions.

Our analysis demonstrated that placental VI^{MV} was not associated with GA in either normal pregnancies or PE cases. Previous studies employing 3D power Doppler with virtual organ computer-aided analysis (VOCAL) technique demonstrated that placental vascularization indices (Vascularization Index, Flow Index, Vascularization Flow Index) were not dependent on GA during mid- and late-trimester [24,25]. Our quantitative analysis revealed a significant reduction in placental VI^{MV} among PE pregnancies compared to normal pregnancies. Previous studies that utilized placental 3D power doppler also showed decreased placental vascularization indices in pregnancies with PE [11,26]. Therefore, despite using different ultrasound techniques, the present study and others have consistently shown that placental vascularization does not change according to the GA. Furthermore, these studies have consistently demonstrated impaired placental vascularization in PE pregnancies, concordant with the pathological feature of placental ischemia in PE [10,11,26].

In early-onset PE cases, we also found that both the RI and PI of the UA and UtAs were significantly higher compared to normal pregnancies at GA $<$34 weeks. In contrast, no significant differences were observed in UtA hemodynamics between late-onset PE cases and GA-matched controls ($\geq$34 weeks), although late-onset PE exhibited elevated RI and PI of the UA. These divergent hemodynamic characteristics between early- and late-onset PE subtypes may be related to different pathogenic mechanisms. Early-onset PE is probably caused by insufficient placentation secondary to failed spiral artery remodeling, manifesting as elevated UtA resistance, whereas late-onset PE is more likely due to an imbalance between decreased placental function and maternal perfusion and fetoplacental demands [8,9].

As previously demonstrated, both early- and late-onset PE cases exhibited significantly higher UA resistance indices compared to GA-matched controls, along with reduced placental microvascular density as evidenced by markedly lower placental VI^{MV}. Together, these findings confirm the pathological microvascular insufficiency characteristic of PE placenta. Notably, UA resistance serves as an indirect indicator of placental hypoperfusion, whereas VI^{MV} provides direct quantitative evidence of microvascular deficiency.

However, our study found no significant differences in placental VI^{MV}-p ($p = 0.170$) or VI^{MV}-m ($p = 0.471$) between early- and late-onset PE cases. This indicates that although the early- and late-onset subtypes have different pathophysiological pathways, both subtypes may have similar impairment of placental perfusion.

The perinatal outcomes of PE pregnancies were also analyzed in this study. In PE cases, no significant differences in placental VI^{MV} were observed between AGA and SGA neonates, suggesting that VI^{MV} may lack predictive value for SGA development in PE pregnancies. Using alternative placental vascular imaging techniques, the existing literature presents conflicting evidence regarding vascular indices and SGA prediction. Some studies reported significant associations between reduced placental vascularization and SGA risk [27,28]. However, consistent with our findings, other investigators [29,30] found that placental vascular indices cannot predict this complication. Therefore, it remains controversial as to whether reduced placental vascularization can predict the risk of SGA newborns.

The primary novelty of our study lies in its application for the first time of MV-Flow imaging to quantitatively evaluate and compare the placental microvasculature between normal and PE pregnancies, and between early- and late-onset PE cases. Other recent studies have employed the microvascular imaging technique of Superb Microvascular Imaging (SMI) to evaluate the placental vascular characteristics [14,20,31–34]. These studies were mainly conducted to evaluate placental microvascularization in normal pregnancy, pregnancy with fetal growth restriction, pregnancy with gestational diabetes, and placenta accreta spectrum [14,20,31–34]. SMI also proved useful for the evaluation of placental microcirculation. However, those SMI studies did not specifically examine differences in the placental microvasculature between normal and PE pregnancy, or between early- and late-onset PE.

Limitations

The present study has several limitations that should be acknowledged. Firstly, the small sample size of the PE group in particular reduced the statistical power of the study and should be considered when interpreting the findings. Nevertheless, as a pilot application of MV-Flow technology in PE, this research provides foundational data for larger studies in the future. Second, to ensure optimal signal quality for the detection of placental microvessels and minimize potential confounding from placental abnormalities, our analysis was restricted to cases with an anterior placenta, and pregnancies with either abnormal placental implantation or umbilical cord anomalies were excluded. While these methodological choices enhanced the internal validity of our study, they excluded many pregnancies and limited the generalizability of our results. Finally, as a single-center investigation, this study may be subject to institutional biases that could affect the accuracy of conclusions. Further multicenter studies with larger cohorts are required to improve the reliability and validity of this research. Additionally, expansion of the inclusion criteria to encompass diverse placental and umbilical cord conditions would enhance the clinical applicability of our findings.

5. Conclusions

MV-Flow imaging enables quantitative assessment of the microvascular architecture in PE placentas. Both early- and late-onset PE pregnancies showed significantly lower placental VI^{MV} compared to normal pregnancies, thus supporting the clinical utility of MV-Flow for evaluation of placental perfusion in PE. Furthermore, no significant difference in placental VI^{MV} was observed between early- and late-onset PE, suggesting similar impairment of placental perfusion in both subtypes.

Availability of Data and Materials

The data that support the findings of this study are available on request from the corresponding author.

Author Contributions

XZ, YF, and LL designed the research study. JP, YG, and XZ performed the research. LM, MH, and JS analyzed the data. All authors contributed to editorial changes in the manuscript. All authors read and approved the final manuscript. All authors have participated sufficiently in the work and agreed to be accountable for all aspects of the work.

Ethics Approval and Consent to Participate

The study was carried out in accordance with the guidelines of the Declaration of Helsinki. The study was approved by the Research Ethics Committee of Shaanxi Provincial People's Hospital (2021213) and written informed consent was obtained from all subjects.

Acknowledgment

Not applicable.

Funding

This work was supported by the Science and Technology Talents Support Project of Shaanxi Provincial People's Hospital (No. 2022JY-22), the Social Development Projects of Science and Technology Department of Shaanxi Province (No. 2022SF-209), the Project of Shaanxi Provincial People's Hospital (No. 2023YJY-62), and the Natural Science Basic Research Program of Science and Technology Department of Shaanxi Province (No. 2025JC-YBQN-1234).

Conflict of Interest

The authors declare no conflict of interest.

References

[1] Spiliopoulos M, Kuo CY, Eranki A, Jacobs M, Rossi CT, Iqbal SN, *et al*. Characterizing placental stiffness using ultrasound shear-wave elastography in healthy and preeclamptic pregnancies. Archives of Gynecology and Obstetrics. 2020; 302: 1103–1112. https://doi.org/10.1007/s00404-020-05697-x.

[2] Chaiworapongsa T, Chaemsaithong P, Yeo L, Romero R. Pre-eclampsia part 1: current understanding of its pathophysiology. Nature Reviews. Nephrology. 2014; 10: 466–480. https://doi.org/10.1038/nrneph.2014.102.

[3] GBD 2013 Mortality and Causes of Death Collaborators. Global, regional, and national age-sex specific all-cause and cause-specific mortality for 240 causes of death, 1990-2013: a systematic analysis for the Global Burden of Disease Study 2013. Lancet. 2015; 385: 117–171. https://doi.org/10.1016/S0140-6736(14)61682-2.

[4] Gestational Hypertension and Preeclampsia: ACOG Practice Bulletin, Number 222. Obstetrics and Gynecology. 2020; 135: e237–e260. https://doi.org/10.1097/AOG.0000000000003891.

[5] Cui H, Yu L, Li H, Wang H, Liang W, Wang H, *et al*. Evaluation of placental growth potential and placental bed perfusion by 3D ultrasound for early second-trimester prediction of preeclampsia. Journal of Assisted Reproduction and Genetics. 2022; 39: 1545–1554. https://doi.org/10.1007/s10815-022-02530-z.

[6] Meler E, Martínez J, Boada D, Mazarico E, Figueras F. Doppler studies of placental function. Placenta. 2021; 108: 91–96. https://doi.org/10.1016/j.placenta.2021.03.014.

[7] Levytska K, Higgins M, Keating S, Melamed N, Walker M, Sebire NJ, *et al*. Placental Pathology in Relation to Uterine Artery Doppler Findings in Pregnancies with Severe Intrauterine Growth Restriction and Abnormal Umbilical Artery Doppler Changes. American Journal of Perinatology. 2017; 34: 451–457. https://doi.org/10.1055/s-0036-1592347.

[8] Burton GJ, Redman CW, Roberts JM, Moffett A. Pre-eclampsia: pathophysiology and clinical implications. BMJ. 2019; 366: l2381. https://doi.org/10.1136/bmj.l2381.

[9] Arbuzova S. Common pathogenesis of early and late preeclampsia: evidence from recurrences and review of the literature. Archives of Gynecology and Obstetrics. 2024; 310: 953–959. https://doi.org/10.1007/s00404-023-07217-z.

[10] Harmon AC, Cornelius DC, Amaral LM, Faulkner JL, Cunningham MW, Jr, Wallace K, *et al*. The role of inflammation in the pathology of preeclampsia. Clinical Science. 2016; 130: 409–419. https://doi.org/10.1042/CS20150702.

[11] Yamasato K, Zalud I. Three dimensional power Doppler of the placenta and its clinical applications. Journal of Perinatal Medicine. 2017; 45: 693–700. https://doi.org/10.1515/jpm-2016-0366.

[12] Hannaford KE, Tuuli M, Goetzinger KR, Odibo L, Cahill AG, Macones G, *et al*. First-trimester 3-dimensional power Doppler placental vascularization indices from the whole placenta versus the placental bed to predict preeclampsia: does pregnancy-associated plasma protein a or uterine artery Doppler sonography help? Journal of Ultrasound in Medicine. 2015; 34: 965–970. https://doi.org/10.7863/ultra.34.6.965.

[13] Chen X, Wei X, Zhao S, Huang H, Wang W, Qiu J, *et al*. Characterization of Placental Microvascular Architecture by MV-Flow Imaging in Normal and Fetal Growth-Restricted Pregnancies. Journal of Ultrasound in Medicine. 2021; 40: 1533–1542. https://doi.org/10.1002/jum.15531.

[14] García-Jiménez R, Arroyo E, Borrero C, Garcia-Mejido JA, Sosa F, Fernández-Palacín A, *et al*. Evaluation of Placental Micro-vascularization by Superb Micro-vascular Imaging Doppler in Cases of Intra-uterine Growth Restriction: A First Step. Ultrasound in Medicine & Biology. 2021; 47: 1631–1636. https://doi.org/10.1016/j.ultrasmedbio.2021.01.029.

[15] Catalano O, Corvino A, Basile L, Catalano F, Varelli C. Use of new microcirculation software allows the demonstration of dermis vascularization. Journal of Ultrasound. 2023; 26: 169–174. https://doi.org/10.1007/s40477-022-00710-2.

[16] Aziz MU, Eisenbrey JR, Deganello A, Zahid M, Sharbidre K, Sidhu P, *et al*. Microvascular Flow Imaging: A State-of-the-

Art Review of Clinical Use and Promise. Radiology. 2022; 305: 250–264. https://doi.org/10.1148/radiol.213303.

[17] Yin SY, Zhu XD, Zhou PP, Xu ZH, Li Q, Jiang TA. Microvascular-Flow Imaging for Assessing Placental Blood Perfusion in the First-Trimester of Pregnancy during the Omicron Epidemic: Correlation with Pregnancy Outcomes. Clinical and Experimental Obstetrics and Gynecology. 2024; 51: 261. https://doi.org/10.31083/j.ceog5112261.

[18] Pomorski M, Zimmer M, Fuchs T, Florjanski J, Pomorska M, Tomialowicz M, *et al*. Quantitative assessment of placental vasculature and placental volume in normal pregnancies with the use of 3D Power Doppler. Advances in Medical Sciences. 2014; 59: 23–27. https://doi.org/10.1016/j.advms.2013.06.002.

[19] González-González NL, González-Dávila E, González Marrero L, Padrón E, Conde JR, Plasencia W. Value of placental volume and vascular flow indices as predictors of intrauterine growth retardation. European Journal of Obstetrics, Gynecology, and Reproductive Biology. 2017; 212: 13–19. https://doi.org/10.1016/j.ejogrb.2017.03.005.

[20] Sainz JA, Carrera J, Borrero C, García-Mejido JA, Fernández-Palacín A, Robles A, *et al*. Study of the Development of Placental Microvascularity by Doppler SMI (Superb Microvascular Imaging): A Reality Today. Ultrasound in Medicine & Biology. 2020; 46: 3257–3267. https://doi.org/10.1016/j.ultrasmedbio.2020.08.017.

[21] Zhu L, Zhang R, Zhang S, Shi W, Yan W, Wang X, *et al*. Chinese neonatal birth weight curve for different gestational age. Chinese Journal of Pediatrics. 2015; 53: 97–103. (In Chinese)

[22] Cavoretto PI, Salmeri N, Candiani M, Farina A. Reference ranges of uterine artery pulsatility index from first to third trimester based on serial Doppler measurements: longitudinal cohort study. Ultrasound in Obstetrics & Gynecology. 2023; 61: 474–480. https://doi.org/10.1002/uog.26092.

[23] Drukker L, Staines-Urias E, Villar J, Barros FC, Carvalho M, Munim S, *et al*. International gestational age-specific centiles for umbilical artery Doppler indices: a longitudinal prospective cohort study of the INTERGROWTH-21st Project. American Journal of Obstetrics and Gynecology. 2020; 222: 602.e1–602.e15. https://doi.org/10.1016/j.ajog.2020.01.012.

[24] Guiot C, Gaglioti P, Oberto M, Piccoli E, Rosato R, Todros T. Is three-dimensional power Doppler ultrasound useful in the assessment of placental perfusion in normal and growth-restricted pregnancies? Ultrasound in Obstetrics & Gynecology. 2008; 31: 171–176. https://doi.org/10.1002/uog.5212.

[25] de Paula CFS, Ruano R, Campos JADB, Zugaib M. Quantitative analysis of placental vasculature by three-dimensional power Doppler ultrasonography in normal pregnancies from 12 to 40 weeks of gestation. Placenta. 2009; 30: 142–148. https://doi.org/10.1016/j.placenta.2008.11.010.

[26] Yuan T, Zhang T, Han Z. Placental vascularization alterations in hypertensive disorders complicating pregnancy (HDCP) and small for gestational age with HDCP using three-dimensional power doppler in a prospective case control study. BMC Pregnancy and Childbirth. 2015; 15: 240. https://doi.org/10.1186/s12884-015-0666-1.

[27] Odibo AO, Goetzinger KR, Huster KM, Christiansen JK, Odibo L, Tuuli MG. Placental volume and vascular flow assessed by 3D power Doppler and adverse pregnancy outcomes. Placenta. 2011; 32: 230–234. https://doi.org/10.1016/j.placenta.2011.01.010.

[28] Hafner E, Metzenbauer M, Stümpflen I, Waldhör T. Measurement of placental bed vascularization in the first trimester, using 3D-power-Doppler, for the detection of pregnancies at-risk for fetal and maternal complications. Placenta. 2013; 34: 892–898. https://doi.org/10.1016/j.placenta.2013.06.303.

[29] Rosner M, Dar P, Reimers LL, McAndrew T, Gebb J. First-trimester 3D power Doppler of the uteroplacental circulation space and fetal growth restriction. American Journal of Obstetrics and Gynecology. 2014; 211: 521.e1–8. https://doi.org/10.1016/j.ajog.2014.05.015.

[30] Farina A. Placental vascular indices (VI, FI and VFI) in intrauterine growth retardation (IUGR). A pooled analysis of the literature. Prenatal Diagnosis. 2015; 35: 1065–1072. https://doi.org/10.1002/pd.4646.

[31] Furuya N, Hasegawa J, Doi M, Koike J, Suzuki N. Accuracy of Prenatal Ultrasound in Evaluating Placental Pathology Using Superb Microvascular Imaging: A Prospective Observation Study. Ultrasound in Medicine & Biology. 2022; 48: 27–34. https://doi.org/10.1016/j.ultrasmedbio.2021.09.002.

[32] Garcia-Jimenez R, Borrero González C, García-Mejido JA, Fernández-Palacín A, Robles A, Sosa F, *et al*. Assessment of late on-set fetal growth restriction using SMI (superb microvascular imaging) Doppler. Quantitative Imaging in Medicine and Surgery. 2023; 13: 4305–4312. https://doi.org/10.21037/qims-22-807.

[33] Çelik AO, Günay B, Çoker GB, Ustabaşıoğlu FE, Ateş S, Tunçbilek N. Evaluation of placenta in patients with gestational diabetes using shear wave elastography and superb microvascular imaging. Acta Radiologica. 2024; 65: 318–323. https://doi.org/10.1177/02841851231217201.

[34] Hasegawa J, Kurasaki A, Hata T, Homma C, Miura A, Kondo H, *et al*. Diagnosis of placenta accreta spectrum using ultra-high-frequency probe and Superb Microvascular Imaging. Ultrasound in Obstetrics & Gynecology. 2019; 54: 705–707. https://doi.org/10.1002/uog.20207.